HHS Public Access

Author manuscript

Cancer Res. Author manuscript; available in PMC 2019 July 01.

Published in final edited form as:

Cancer Res. 2018 July 01; 78(13): 3510–3521. doi:10.1158/0008-5472.CAN-17-3592.

MIR142 loss-of-function mutations derepress ASH1L to increase HOXA gene expression and promote leukemogenesis

Maria C. Trissal[1], **Terrence N. Wong**[1], **Juo-Chin Yao**[1], **Rahul Ramaswamy**[1], **Iris Kuo**[1], **Jack Baty**[2], **Yaping Sun**[3], **Gloria Jih**[4], **Nishi Parikh**[4], **Melissa M. Berrien-Elliott**[1], **Todd A. Fehniger**[1], **Timothy J. Ley**[1], **Ivan Maillard**[3,4,5], **Pavan R. Reddy**[3], and **Daniel C. Link**[1]

[1]Division of Oncology, Washington University School of Medicine, St. Louis, Missouri

[2]Division of Biostatistics, Washington University, St. Louis, Missouri

[3]Division of Hematology-Oncology, University of Michigan, Ann Arbor, Michigan

[4]Life Sciences Institute, University of Michigan, Ann Arbor, Michigan

[5]Department of Cell and Developmental Biology, University of Michigan, Ann Arbor, Michigan

Abstract

Point mutations in the seed sequence of miR-142-3p are present in a subset of AML and in several subtypes of B cell lymphoma. Here we show that mutations associated with AML result both in loss of miR-142-3p function and in decreased miR-142-5p expression. *Mir142* loss altered the hematopoietic differentiation of multipotent hematopoietic progenitors, enhancing their myeloid potential while suppressing their lymphoid potential. During hematopoietic maturation, loss of *Mir142* increased Ash1l protein expression and consequently resulted in the aberrant maintenance of *Hoxa* gene expression in myeloid-committed hematopoietic progenitors. *Mir142* loss also enhanced the disease-initiating activity of *IDH2* mutant hematopoietic cells in mice. Together these data suggest a novel model in which miR-142, through repression of ASH1L activity, plays a key role in suppressing *HOXA9/A10* expression during normal myeloid differentiation. AML-associated loss-of-function mutations of *MIR142* disrupt this negative signaling pathway, resulting in sustained *HOXA9/A10* expression in myeloid progenitors/myeloblasts and ultimately contributing to leukemic transformation.

INTRODUCTION

MicroRNAs (miRNAs) are non-coding RNAs, which inhibit the expression of messenger RNAs (mRNAs) (1). MiRNA genes are transcribed as primary miRNAs, which are processed by the Drosha microprocessor complex into precursor miRNAs. Precursor miRNAs are processed by Dicer, generating a duplex, which contains two distinct mature miRNA species, referred to as 5p or 3p depending on whether they are derived from the 5′ or 3′ end of the primary transcript. Only one strand is loaded into the RNA induced

Corresponding Author: Daniel C. Link, Washington University School of Medicine, 660 South Euclid Avenue, Campus Box 8007, St Louis, MO 63110; Phone: 314-362-8871; Fax: 314-362-9333; danielclink@wustl.edu.
M.C. Trissal, T.N. Wong, and J-C. Yao contributed equally to this article.

Disclosure of Potential Conflicts of Interest: No potential conflicts of interest were disclosed.

silencing complex (RISC); the other is discarded. The incorporated strand guides the RISC to semi-complementary mRNA targets and inhibits their expression by either directly repressing translation or promoting mRNA decay (2). A miRNA can target hundreds of mRNAs based on sequence complementarity.

There is evidence that the dysregulation of certain miRNAs contributes to leukemogenesis. For example, *MIR125* overexpression, due to the rare chromosomal translocation t(2:11)(p21;p23) or through epigenetic mechanisms, promotes leukemogenesis in mouse models (3). The genetic loss or epigenetic silencing of miRNAs also has been implicated in AML pathogenesis. For example, the loss of *MIR145* and *MIR146A* in myeloid neoplasms carrying 5q chromosomal deletions has been shown to contribute to AML (4). In contrast, genetic alterations solely targeting miRNAs are uncommon in AML (5). In the TCGA cohort of 200 AML patients, *MIR142* was the only recurrently mutated miRNA (6). *MIR142* point mutations were identified in 4 cases, with one case bi-allelic; all mutations localized to the miR-142-3p seed sequence. A subsequent study produced similar results (7). *MIR142* is also mutated in follicular and diffuse large B cell lymphoma at reported frequencies of 10–25% and 12–20% respectively (8–11). These mutations also often localize to the miR-142-3p seed sequence.

MIR142 is highly-conserved and broadly expressed in mature hematopoietic cells (12,13). It is expressed at lower levels in hematopoietic stem/progenitor cells (HSPCs). In mice, *Mir142* loss results in splenomegaly from an expansion of myeloid and $CD19^+$ B cells (14,15). *Mir142* loss is also associated with the impaired development and function of multiple hematopoietic lineages, including B1 B cells (14), T cells (16,17), $CD4^+$ dendritic cells (15), mast cells (18), megakaryocytes (19), and erythroid precursors (20,21). MiR-142's role in regulating HSPCs is less well defined, although inhibition of miR-142-3p in zebrafish results in reduced HSPC activity (22).

Here, we show that AML-associated *MIR142* mutations disrupt miR-142-3p function and result in decreased miR-142-5p expression. In mice, *Mir142* loss enhances the myeloid potential, while suppressing the lymphoid potential, of multipotent HSPCs. Moreover, *Mir142* loss enhances the disease initiating capacity of $IDH2^{R172K}$ mutant hematopoietic cells. We provide evidence that these phenotypes are due, in part, to derepression of Ash1l (absent, small, or homeotic 1-like), a histone methyltransferase, which positively regulates *Hoxa* gene expression. These data suggest a novel model in which *MIR142* mutations, through derepression of ASH1L, cause sustained *HOXA9/A10* expression during myeloid differentiation, ultimately contributing to leukemic transformation.

MATERIALS AND METHODS

Patient Studies

Bone marrow samples from patients with AML were collected as part of a single-institution banking protocol approved by the Washington University Human Studies Committee (IRB#01-1014). Healthy donor bone marrow samples were obtained following written informed consent as approved by the Washington University Institutional Review Board. All patient studies were performed in accordance with the Declaration of Helsinki.

Mouse models

Mice were maintained under standard pathogen-free conditions with animal studies conducted in accordance with IACUC-approved Washington University protocols. Mice on a C57Bl/6 background with homozygous deletion of *Mir142* (*Mir142*$^{-/-}$) were generated and described by Sun et al. (17). Mice on a C57Bl/6 background with a gene trap insertion cassette causing >90% reduction of full length *Ash1l* transcript (*Ash1l*$^{GT/GT}$) were generated and described by Jones et al. (23). Experimental and control mice were age (8–12 weeks) and sex-matched.

Cell lines and cell culture

HEK293T cells were obtained from ATCC and cultured in a humidified incubator at 37°C with 5% CO_2. They were maintained in Dulbecco's Modified Eagle Medium (Gibco) with 10% fetal bovine serum (Atlas), penicillin (100 Units/ml) (Gibco) and streptomycin (100 μg/ml) (Gibco). Cells were passaged upon reaching a confluency of 75–80% with Trypsin-EDTA (0.25%) (Gibson). HEK293T cells were not authenticated or tested for Mycoplasma and were used within 3–5 passages after initial expansion.

RNA expression in murine hematopoietic populations

The NucleoSpin RNA kit (Macherey-Nagel) was used to isolate RNA from CD150^{+}CD48^{-}c-kit^{+}Sca1^{+}lineage^{-} cells. For other populations, RNA was isolated with Trizol LS (Thermo Fisher). RNA expression was assessed with two-step RT-qPCR using iScript reverse transcriptase (Bio-Rad) and iTaq DNA polymerase (Bio-Rad).

Protein extraction

To isolate histones, bone marrow c-kit^{+}-selected cells were isolated with CD117 MicroBeads on the autoMACS Pro Separator (Miltenyi). They were washed twice with PBS and lysed in a PBS solution with 0.5% Triton X-100 (Sigma), 2 mM PMSF (Sigma), and 0.02% sodium azide (Sigma). After 10 minutes on ice, samples were centrifuged at 2,000 rpm for 10 minutes at 4°C. The pellets were resuspended in 0.2N HCl and histones extracted at 4°C overnight. Finally, samples were centrifuged at 2,000 rpm for 10 minutes at 4°C and the histone-containing supernatant collected.

To isolate ASH1L, 2x10^{6} bone marrow cells were washed twice with PBS and lysed in a buffer consisting of 7M urea (Sigma), 2M thiourea (Sigma), 4%CHAPS (Sigma), 30 mM Tris (Sigma), and a protease inhibitor cocktail (Thermo Fisher). To prepare for Western blotting, the solution was frozen and thawed three times on dry ice, dissolved in Laemmli buffer, heated at 99°C for 5 minutes, and sonicated.

Viral transduction and bone marrow transplantation

For competitive transplantation, bone marrow cells from *Mir142*$^{+/+}$ or *Mir142*$^{-/-}$ Ly5.2 mice were mixed with competitor wild type bone marrow cells expressing Ly5.1 and retro-orbitally transplanted into lethally irradiated (1000 cGy) Ly5.1/5.2 recipient mice.

For transplantation of phenotypic stem cells, 20–25 CD150^{+}CD48^{-}c-kit^{+}Sca1^{+} lineage^{-} cells from *Mir142*$^{+/+}$ or *Mir142*$^{-/-}$ Ly5.2 mice were sorted into individual wells containing

2.5–3x10^5 support bone marrow cells (Ly5.1 or Ly5.1/Ly5.2) and injected retro-orbitally into lethally irradiated (1000 cGy) recipient mice (Ly5.1 or Ly5.1/Ly5.2). The lineage output of the transplanted HSCs was determined 24 weeks post-transplantation in the peripheral blood of mice with identifiable Ly5.2 engraftment in both myeloid ($Gr1^+$ or $CD115^+$) and lymphoid ($B220^+$ or $CD3^+$) lineages.

Human *IDH2*^{R172K} over-expression was achieved using an MSCV-IRES-mcherry vector (Addgene #52114). HEK293T cells were transfected with the retroviral vector and an Ecopak plasmid (Addgene #12371) using the Calcium Phosphate Transfection Kit (Thermo Fisher). Viral supernatant collected 48 hours post-transfection was added to bone marrow c-kit^+ cells that were isolated using CD117 MicroBeads on the autoMACS Pro Separator and cultured in MEMα (Gibco) with 15% fetal bovine serum (Atlas) and a cytokine cocktail (TPO 10 ng/mL, IL-3 10 ng/mL, SCF 100 ng/mL, and Flt3-L 50 ng/mL; Peprotech). Cells were centrifuged at 966xg for 90 minutes at 30°C and incubated at 37°C overnight. Viral transduction was repeated the following day. 2–3x10^5 cells were injected retro-orbitally into lethally irradiated (1000 cGy) mice. Mice were followed and sacrificed if they became symptomatic from either hematologic or non-hematologic etiologies, had a hemoglobin <5 g/dl, or reached the end of the follow-up period (>1 year). Mice were censored if they were sacrificed for non-hematologic reasons or reached the end of the follow-up period.

For secondary transplantation, one million splenocytes from sacrificed mice previously transplanted with single mutant *IDH2*^{R172K} or double mutant *Mir142*$^{-/-}$ *IDH2*^{R172K} cells were injected retro-orbitally into sublethally irradiated (650 cGy) mice.

Statistical Analyses

Data is represented as the mean ± standard error of the mean with relevant statistical tests noted in the figure legends.

Data availability

Small RNA sequencing data from AML samples were submitted to dbGaP (accession number phs000159.v9). All other relevant data are included in the article or supplementary files, or available from the authors upon request.

RESULTS

MIR142 mutations attenuate miR-142-3p and miR-142-5p function

All *MIR142* mutations in the TCGA AML cohort localized to the miR-142-3p seed sequence (Fig 1A). MiRNA target prediction programs (mirdb.org) suggested that all three mutations would cause a loss of most 3p targets with no commonly gained targets shared amongst all three mutants. As expected, both the A55G and G58C *MIR142* mutants were unable to inhibit translation in a luciferase assay using the 3′ untranslated regions (UTRs) of the known miR-142-3p targets *RAC1* (24,25) and *TGFBR1* (26) (Fig 1B–C), indicating that AML-associated *MIR142* mutations disrupt its 3p function.

Interestingly, overexpression of the A55G and G58C mutant MIR142 hairpins resulted in significantly reduced levels of mature 5p compared to wild type, despite these mutations

being localized to 3p (Suppl. Fig 1A). In contrast, levels of the mutant 3p strand derived from these hairpins were similar or increased when compared to wild type, resulting in a reduced 5p:3p ratio (Suppl. Fig 1B). Expression of the mutant MIR142 precursors was similar to that of wild type (Suppl. Fig 1C). Thermodynamic stability at the 5′ end of miRNAs within the small RNA duplex influences miRNA loading into the RISC; the strand with decreased stability towards its 5′ end is preferentially loaded (27). Theoretically, AML-associated *MIR142* mutations should decrease stability at the 5′ end of 3p, causing its preferential loading at 5p's expense. To test this, we assessed the levels of RISC-associated miR-142-5p and miR-142-3p. Indeed overexpression of the A55G and G58C mutant MIR142 hairpins resulted in decreased RISC-associated miR-142-5p compared to wild type and a reduced 5p:3p ratio (Fig 1D–E).

We then assessed miR-142-5p and miR-142-3p expression in AML with or without *MIR142* mutations. Consistent with prior reports (28), compared with healthy donor $CD34^+$ cells, miR-142-5p and 3p expression were on average 16 and 31-fold higher respectively in AML (Suppl. Fig 1D). In both AML with wild type *MIR142* and in normal $CD34^+$ cells, 5p had slightly higher expression than 3p (Fig 1F & Suppl. Fig 1E). However, in the four *MIR142* mutated AMLs, we observed significantly decreased expression of 5p relative to 3p. This was most striking in the AML with bi-allelic *MIR142* mutations where 5p levels were markedly reduced. Collectively, these data show that AML-associated *MIR142* mutations cause both loss of miR-142-3p function and reduced RISC incorporation and stability of miR-142-5p.

Mir142 loss alters hematopoietic differentiation

Since AML-associated *MIR142* mutations cause a functional loss of both miR-142-3p and 5p, we assessed hematopoiesis in $Mir142^{-/-}$ mice. As reported previously, these mice were leukopenic (19,29), primarily due to a loss of T cells and to a lesser extent of B cells (Fig 2A & Suppl. Fig 2A–B). They also exhibited splenomegaly, with an increased number of mature granulocytes and B cells and a reduced number of T cells (Fig 2B & Suppl. Fig 2C–D) (14,15). In contrast, the bone marrow cellularity of $Mir142^{-/-}$ mice was similar to wild type, with a similar percentage of neutrophils, monocytes, and B cells (Fig 2C & Suppl. Fig 2E–2F). Although at baseline $Mir142^{-/-}$ mice had normal red blood cell and platelet parameters (Suppl. Fig 2G–I), they exhibited a significant decrease in both bone marrow megakaryocyte-erythrocyte progenitors (MEPs) and erythroid progenitors, consistent with a recent report (Fig 2D–F) (20). In contrast, the percentage of granulocyte-monocyte progenitors (GMPs) and common myeloid progenitors (CMPs) in the bone marrow of $Mir142^{-/-}$ mice was similar to wild type (Fig 2D).

We asked whether *Mir142* loss alters multipotent hematopoietic progenitors (MPPs). We observed a modest increase in $Kit^+Sca^+lineage^-$ (KSL) cells in $Mir142^{-/-}$ mice (Fig 3A). As previously described (30), MPPs can be analyzed based on CD34, CD48, CD135, and CD150 expression (Suppl. Fig 3A). We found that the KSL expansion in $Mir142^{-/-}$ mice was due to an increase in myeloid-biased MPP3 ($CD150^-CD48^+CD34^+CD135^-$) cells (Fig 3B). The percentage of phenotypic HSCs ($CD150^+CD48^-$KSL cells) in the bone marrow was similar in $Mir142^{-/-}$ and wild type mice (Fig 3C). CD229 surface expression

discriminates between lymphoid-biased and more myeloid-biased HSCs, with most HSCs being lymphoid-biased and expressing CD229 in young mice (31). However, in *Mir142*$^{-/-}$ mice, most phenotypic HSCs had low CD229 expression, suggesting a loss of lymphoid potential (Fig 3D–E). Interestingly, a modest decrease in HSC quiescence was observed in *Mir142*$^{-/-}$ mice (Fig 3F). These data suggest that *Mir142* loss not only alters differentiation in mature hematopoietic populations but also in immature HSPC populations, resulting in a loss of erythroid and lymphoid potential while maintaining myeloid potential.

Mir142$^{-/-}$ bone marrow exhibits reduced repopulating activity with a loss of HSC lymphoid potential

We next assessed HSC function through transplantation experiments. Whole bone marrow competitive repopulation assays showed a modest repopulating defect with *Mir142*$^{-/-}$ bone marrow (Fig 4A). Post-transplantation, *Mir142*$^{-/-}$ cells had reduced contribution to the bone marrow myeloid, lymphoid, and HSPC populations (Fig 4B). Consistent with the phenotype of *Mir142*$^{-/-}$ mice, the reduction was more pronounced in lymphoid versus myeloid cells, suggesting that *Mir142*$^{-/-}$ HSCs may be deficient in lymphoid potential. To address this, we performed transplantation experiments with a limited number of CD150^{+}CD48^{-}KSL cells. As expected, since young (8–10 week-old) donor mice were used, the majority of wild type HSCs primarily contributed to the lymphoid lineages (Fig 4C). In contrast, *Mir142*$^{-/-}$ HSCs contributed more significantly to the myeloid lineages (Fig 4D–E). As *Mir142* is essential for proper T cell development, we repeated this analysis excluding T cells; again, *Mir142*$^{-/-}$ HSCs contributed more significantly to the myeloid lineages (Suppl. Fig 4A–C). Using the previously described GM:(B+T) ratio (32), wild type HSCs were more likely to be lymphoid-biased, with *Mir142*$^{-/-}$ HSCs more likely to be myeloid-biased or balanced (Fig 4F). These data show that *Mir142* loss results in a modest decrease in total bone marrow repopulating activity with a loss of HSC lymphoid potential.

Mir142 loss increases *Hoxa9/a10* expression through derepression of Ash1l

ASH1L was identified as a miR-142 target in thyroid neoplasias (33), with two putative miR-142-5p and five putative miR-142-3p binding sites in its 3′ UTR (Fig. 5A). ASH1L is a member of the trithorax family of histone methyltransferases and is linked to the trimethylation of histone 3 lysine 4 (H3K4me3) (34) and the dimethylation of histone 3 lysine 36 (H3K36me2) (35). In hematopoiesis, ASH1L is essential for maintenance of HSC self-renewal (23) and plays a key role in *MLL*-induced leukemogenesis (36). In hematopoietic cell lines, *ASH1L* knockdown promotes erythropoiesis while inhibiting granulopoiesis (37). These observations suggest that loss of miR-142-mediated suppression of Ash1l activity in *Mir142*$^{-/-}$ mice may contribute to their hematopoietic phenotype.

To test this hypothesis, we first assessed the ability of *MIR142* hairpins to suppress protein expression in a luciferase assay using *ASH1L*'s 3′ UTR (Fig. 5B). Wild type *MIR142* decreased the luciferase signal by >80%. In contrast, the A55G and G58C mutant hairpins didn't suppress luciferase activity. Ash1l protein levels were increased ~three-fold in total bone marrow cells from *Mir142*$^{-/-}$ mice compared to wild type, confirming miR-142's importance in suppressing Ash1l protein expression *in vivo* (Fig. 5C). Interestingly, *Ash1l* mRNA expression was increased in *Mir142*$^{-/-}$ c-kit^{+}-selected bone marrow cells, suggesting

that miR-142 also regulates *Ash1l* mRNA levels by promoting its decay (Fig. 5D). To determine the consequences of Ash1l overexpression, we interrogated global histone modification levels in c-kit$^+$-selected bone marrow cells. Consistent with Ash1l's function as an H3K36 dimethyltransferase, global H3K36me2 levels were increased two-fold in *Mir142*$^{-/-}$ cells compared to wild type; other histone modification marks (H3K36me3 and H3K27me3) were unchanged (Fig 5E–F).

ASH1L is an important positive regulator of *HOX* gene expression (34,35,37). During murine hematopoietic differentiation, *Ash1l* and *Hoxa9/a10* exhibit a similar pattern of mRNA expression, with high expression in HSCs and a progressive decline with differentiation (Fig 6A–C). In contrast, *Mir142* is expressed at lower levels in HSCs, increasing in expression in more mature populations (Fig 6D). As miR-142 suppresses Ash1l activity in hematopoietic cells, we hypothesized that it may contribute to the decrease in *Hoxa9/a10* mRNA expression during hematopoietic differentiation. To test this, we measured *Hoxa9/a10* expression in sorted *Mir142*$^{-/-}$ hematopoietic populations. As expected, *Mir142* loss did not affect *Hoxa9/a10* expression in HSCs. However, we observed a significant increase in *Hoxa9/a10* expression in both *Mir142*$^{-/-}$ myeloid committed progenitors and total bone marrow cells (Fig 6E–F).

We next measured histone modifications at the *Hoxa9* promoter. We focused on H3K4 trimethylation and H3K36 dimethylation as Ash1l is implicated in the regulation of these histone modifications. H3K4me3 and H3K36me2 (but not H3K36me3) occupancy at the *Hoxa9* promoter was increased in *Mir142*$^{-/-}$ c-kit$^+$ bone marrow cells when compared to wild type (Figure 6G–I). Collectively, these data suggest that *Mir142* loss results in increased *Hoxa9* expression through enhanced Ash1l activity. To test this, we crossed *Mir142*$^{-/-}$ mice with *Ash1l* deficient mice (*Ash1l*$^{GT/GT}$). *Ash1l*$^{GT/GT}$ mice have a gene trap insertion cassette following exon 1 of *Ash1l*, causing a >90% reduction in its full-length transcript (23). We then assessed *Hoxa9* expression in total bone marrow cells (Fig 6J). As previously demonstrated, *Mir142*$^{-/-}$ mice had significantly increased *Hoxa9* expression compared to wild type. As reported previously, *Ash1l*$^{GT/GT}$ mice had slightly decreased *Hoxa9* expression. In double mutant *Mir142*$^{-/-}$*Ash1l*$^{GT/GT}$ mice, the effect of *Mir142* loss on *Hoxa9* expression was abrogated, showing that miR-142 regulates *Hoxa9* expression primarily by repressing Ash1l activity.

Mir142 loss enhances *IDH2*^{R172K} disease-initiating capacity

In the TCGA AML cohort, all *MIR142* mutant patients harbored mutations in *IDH1* or *IDH2* (6). To determine whether *MIR142* loss cooperates with *IDH* mutations to induce AML, we reconstituted lethally irradiated mice with wild type or *Mir142*$^{-/-}$ c-kit$^+$-selected cells transduced with a retrovirus expressing human *IDH2*^{R172K}. As reported previously (38,39), mice transplanted with wild type cells expressing *IDH2*^{R172K} developed a fatal myelodysplastic-like phenotype characterized by anemia, thrombocytopenia, splenomegaly, bone marrow hypocellularity, and a variable white blood cell count (Fig 7A, Suppl. Fig 5A–E). Concomitant loss of *Mir142* did not affect the latency or penetrance of this disorder (Fig. 7A). However, consistent with the *Mir142*$^{-/-}$ phenotype, double mutant mice had a significantly more severe anemia (Fig 7B). They also exhibited increased hematopoietic

immaturity with a higher percentage of myeloid blasts in the bone marrow, blood, and spleen (Fig 7C–D, Suppl. Fig 5F). In fact, 11/15 (73.3%) of double mutant mice exceeded the 20% myeloblasts diagnostic threshold for AML, compared to only 1/7 (14.3%) mice expressing *IDH2*^{R172K} alone ($P<0.05$ by Fisher's Exact Test). Mice transplanted with wild type or *Mir142*$^{-/-}$ cells lacking *IDH2*^{R172K} expression did not develop a progressive hematologic disorder.

Previous studies showed that *Hoxa9* overexpression cooperates with *Idh* mutations to induce a myeloproliferative-like disorder in mice (38,40,41). Since *Mir142* loss is associated with increased *Hoxa9/a10* expression, we measured expression of these two genes in total bone marrow cells from *IDH2*^{R172K} or *IDH2*^{R172K}*Mir142*$^{-/-}$ mice. *IDH2*^{R172K} expression alone did not cause increased *Hoxa9/a10* expression (Fig 7E). In contrast, both *Hoxa9* and *Hoxa10* expression were significantly increased in *IDH2*^{R172K}*Mir142*$^{-/-}$ cells. Increased *Hoxa9/a10* expression also was observed in flow-sorted CD34^{+} cells from *IDH2*^{R172K}*Mir142*$^{-/-}$ mice compared to *IDH2*^{R172K} mice (Fig 7F).

Increased *Hoxa9/a10* expression has been linked to enhanced self-renewal in hematopoietic cells (42,43). Thus, we asked whether *Mir142* loss increased the ability of *IDH2*^{R172K} mutant hematopoietic cells to initiate disease following transplantation. We transplanted one million splenocytes from single (*IDH2*^{R172K} alone) or double mutant mice exhibiting the previously described phenotype into sub-lethally irradiated recipients. Whereas cells from most single mutant donors failed to engraft, cells from all double mutant donor mice engrafted at varying efficiency (Fig 7G). Engrafted mice developed a similar phenotype to their donors, exhibiting anemia, splenomegaly, and hematopoietic immaturity (Fig 7H–J). Collectively, these data suggest that *Mir142* loss increases the disease-initiating activity of *IDH2*^{R172K} mutant hematopoietic cells.

DISCUSSION

In this study, we show that AML-associated *MIR142* mutations disrupt miR-142-3p's ability to inhibit expression of its target genes. Moreover, by altering the preference for which miRNA strand is incorporated into the RISC, they also decrease miR-142-5p levels. This may be applicable to other miRNA mutations. Any mutation disrupting Watson Crick base pairing at the ends of the miRNA duplex may influence the preferential loading of one miRNA strand versus the other. In the TCGA sequencing of solid malignancies, somatic mutations were identified in the 5p and 3p seed sequence of multiple miRNAs (44). In a significant fraction of cases, the more highly expressed miRNA strand was the non-mutated strand (http://www.mirbase.org). In these cases, the primary effect of these mutations may be to reduce expression of the opposite strand.

To model the effect of miR-142-3p seed sequence mutations, we characterized hematopoiesis in *Mir142*$^{-/-}$ mice. We confirmed prior studies showing that *Mir142* loss results in multiple hematopoietic alterations, including myeloid expansion, impaired erythropoiesis, and T cell lymphopenia. However, we also show that *Mir142* plays a role in the function and lineage determination of multipotent HSPCs. In *Mir142*$^{-/-}$ mice, total bone marrow repopulating activity and HSC quiescence is modestly reduced. Among multipotent

progenitors, there is an expansion of myeloid-biased MPP3 cells. Transplantation studies using a small number of phenotypic HSCs provide evidence that *Mir142*$^{-/-}$ HSCs have reduced lymphoid potential. Thus, although *Mir142* is expressed at lower levels in HSPCs, it contributes to their function.

Our data show miR-142 to be a key post-transcriptional regulator of Ash1l in hematopoietic cells, with increased Ash1l expression and activity in *Mir142*$^{-/-}$ mice. *Ashl1* is a key positive regulator of *Hoxa* gene family expression, whose loss results in a decline of functional HSCs (23). Our data suggest that *Mir142* limits *Hoxa* gene expression during hematopoietic differentiation by suppressing Ash1l activity. *Mir142* loss had no effect on *Hoxa9/a10* expression in HSCs but caused a significant increase in *Hoxa9/a10* expression in myeloid committed and total bone marrow cells. Of note, enforced expression of *Hoxa9* or *Hoxa10* phenocopies some of the hematopoietic alterations in *Mir142*$^{-/-}$ mice, including myeloid expansion and impaired lymphopoiesis and erythropoiesis (43,45). However, not all hematopoietic abnormalities in *Mir142*$^{-/-}$ mice can be explained by Ash1l overexpression. For example, *Ash1l* loss results in a marked reduction in HSCs (23). Increased *Ash1l* expression in HSPCs would not explain the modest loss of *Mir142*$^{-/-}$ total bone marrow repopulating activity. *Mir142* target genes contributing to the altered functionality and reduced lymphoid potential of *Mir142*$^{-/-}$ HSCs require further investigation.

Hoxa gene family expression is essential for normal HSC function. HSCs lacking specific *Hoxa* genes have an impaired ability to respond to stress and reduced repopulating ability (42). Conversely, enforced expression of specific *Hoxa* genes results in HSC expansion and a transplantable myeloproliferative phenotype (43,46). Certain oncogenes (e.g. *MLL* translocations) directly induce *HOX* expression (47). In most AMLs, the cause of elevated *HOX* expression remains unclear. Many AML subtypes have a similar *HOX* expression pattern to normal CD34^{+} cells, suggesting that, in these AMLs, *HOX* genes aren't actively dysregulated but instead "captured" in their normal stem cell state (48). The mechanisms through which stem-cell-like *HOX* expression patterns are maintained in myeloblasts are largely unknown. We provide evidence that *MIR142* loss-of-function mutations, by derepressing ASH1L, represent a novel mechanism of increased *HOXA* gene expression in AML.

We show that *MIR142* loss isn't sufficient to induce leukemia, indicating that additional leukemia-initiating events are required. All four *MIR142* mutant AMLs in the TCGA cohort carried mutations in *IDH1* or *IDH2*. Our data suggest that concomitant *Mir142* loss enhances the disease-initiating activity of *IDH2*^{R172K} mutant hematopoietic cells. In mice, *Hoxa9* overexpression cooperates with *IDH1/2* mutations and their oncogenic metabolite (R)-2-hydroxyglutarate to promote leukemogenesis Our data suggest that *MIR142* loss enhances the disease-initiating activity of *IDH2*^{R172K} mutant hematopoietic cells through derepression of ASH1L and increased *HOXA* gene expression. Unlike other leukemia drivers, *IDH* mutations are rarely observed in clonal hematopoiesis and haven't been shown to provide a fitness advantage upon transplantation. It is possible that *IDH* mutations do not by themselves provide a self-renewal advantage and require the maintenance of *HOX* expression for leukemic transformation. This is consistent with data showing that mutant *IDH1/2* expression in mice doesn't result in enhanced HSC self-renewal (38,41) and with

our data showing that the MDS-like disorder induced by retroviral overexpression of *IDH2*^{R172K} is not highly transplantable.

MIR142 mutations are rare in AML, occurring in 0.5–2% of patients in several cohorts (6,7) and not identified in other series (49). Consistent with our hypothesis that loss of *MIR142* results in sustained *HOXA9/A10* expression, all three *MIR142*-mutated AMLs in the TCGA cohort for whom RNA sequencing was available had *HOXA9* expression >1.0 by FPKM (6). However, high *HOXA9/A10* expression was observed in most *IDH1/2*-mutated AMLs, regardless of *MIR142* mutation status. As our data suggests that *IDH* mutations do not independently promote *HOX* expression, other mechanisms likely contribute to sustained *HOXA9/10* expression in these cases.

In summary, we show that AML-associated *MIR142* mutations cause functional loss of miR-142-3p and miR-142-5p. In mice, *Mir142* loss results in altered HSC function with reduced lymphoid potential and enhances the disease initiating capacity of *IDH2* mutant hematopoietic cells. *Mir142* loss causes derepression of Ash1l, resulting in the inappropriate maintenance of *Hoxa9/a10* gene expression during hematopoietic differentiation. Thus, AML-associated *MIR142* mutations may contribute to leukemogenesis by increasing *HOXA* gene expression in myeloid-committed progenitors. Given the importance of *HOXA* expression in maintaining self-renewal, targeting these pathways (e.g. by inhibiting ASH1L methyltransferase activity) may have therapeutic benefit against AML.

Supplementary Material

Refer to Web version on PubMed Central for supplementary material.

Acknowledgments

This work was supported by National Institutes of Health, National Cancer Institute grants PO1 CA101937 (D.C. Link & T.J. Ley), P50 CA171963 (D.C. Link), K08 CA197369 (T.N. Wong), T32 CA113275 (J.C. Yao), and F32 CA200253 (M.M. Berrien-Elliott), by National Institutes of Health, National Heart, Lung, and Blood Institute grants T32 HL7088-37 (M.C. Trissal) and K12 HL087107 (T.N. Wong), by National Institutes of Health, National Institute on Aging grant R01 AG050509 (I.P. Maillard), by National Institutes of Health, National Institute of Allergy and Infectious Diseases grant R01 AI102924 (T.A. Fehniger), and by the University of Michigan Organogenesis Training Program grant T32 HD007505 (G. Jih). Technical support was provided by the Alvin J. Siteman Cancer Center Tissue Procurement Core and the High-Speed Cell Sorting Core at Washington University School of Medicine, which are supported by National Institutes of Health, National Cancer Institute grant P30 CA91842.

The authors thank Amy P. Schmidt for technical assistance and Jackie Tucker-Davis for animal care.

References

1. Kim VN. MicroRNA biogenesis: coordinated cropping and dicing. Nat Rev Mol Cell Biol. 2005; 6:376–85. [PubMed: 15852042]
2. Iwakawa HO, Tomari Y. The Functions of MicroRNAs: mRNA Decay and Translational Repression. Trends Cell Biol. 2015; 25:651–65. [PubMed: 26437588]
3. Shaham L, Binder V, Gefen N, Borkhardt A, Izraeli S. MiR-125 in normal and malignant hematopoiesis. Leukemia. 2012; 26:2011–8. [PubMed: 22456625]
4. Starczynowski DT, Kuchenbauer F, Argiropoulos B, Sung S, Morin R, Muranyi A, et al. Identification of miR-145 and miR-146a as mediators of the 5q- syndrome phenotype. Nat Med. 2010; 16:49–58. [PubMed: 19898489]

5. Ramsingh G, Jacoby MA, Shao J, De Jesus Pizzaro RE, Shen D, Trissal M, et al. Acquired copy number alterations of miRNA genes in acute myeloid leukemia are uncommon. Blood. 2013; 122:e44. [PubMed: 24009227]
6. Ley TJ, Miller C, Ding L, Raphael BJ, Mungall AJ, et al. Cancer Genome Atlas Research N. Genomic and epigenomic landscapes of adult de novo acute myeloid leukemia. N Engl J Med. 2013; 368:2059–74. [PubMed: 23634996]
7. Thol F, Scherr M, Kirchner A, Shahswar R, Battmer K, Kade S, et al. Clinical and functional implications of microRNA mutations in a cohort of 935 patients with myelodysplastic syndromes and acute myeloid leukemia. Haematologica. 2015; 100:e122–4. [PubMed: 25552704]
8. Bouska A, Zhang W, Gong Q, Iqbal J, Scuto A, Vose J, et al. Combined copy number and mutation analysis identifies oncogenic pathways associated with transformation of follicular lymphoma. Leukemia. 2017; 31:83–91. [PubMed: 27389057]
9. Hezaveh K, Kloetgen A, Bernhart SH, Mahapatra KD, Lenze D, Richter J, et al. Alterations of microRNA and microRNA-regulated messenger RNA expression in germinal center B-cell lymphomas determined by integrative sequencing analysis. Haematologica. 2016; 101:1380–9. [PubMed: 27390358]
10. Kwanhian W, Lenze D, Alles J, Motsch N, Barth S, Doll C, et al. MicroRNA-142 is mutated in about 20% of diffuse large B-cell lymphoma. Cancer Med. 2012; 1:141–55. [PubMed: 23342264]
11. Morin RD, Assouline S, Alcaide M, Mohajeri A, Johnston RL, Chong L, et al. Genetic Landscapes of Relapsed and Refractory Diffuse Large B-Cell Lymphomas. Clin Cancer Res. 2016; 22:2290–300. [PubMed: 26647218]
12. Merkerova M, Belickova M, Bruchova H. Differential expression of microRNAs in hematopoietic cell lineages. Eur J Haematol. 2008; 81:304–10. [PubMed: 18573170]
13. Petriv OI, Kuchenbauer F, Delaney AD, Lecault V, White A, Kent D, et al. Comprehensive microRNA expression profiling of the hematopoietic hierarchy. Proc Natl Acad Sci U S A. 2010; 107:15443–8. [PubMed: 20702766]
14. Kramer NJ, Wang WL, Reyes EY, Kumar B, Chen CC, Ramakrishna C, et al. Altered lymphopoiesis and immunodeficiency in miR-142 null mice. Blood. 2015; 125:3720–30. [PubMed: 25931583]
15. Mildner A, Chapnik E, Manor O, Yona S, Kim KW, Aychek T, et al. Mononuclear phagocyte miRNome analysis identifies miR-142 as critical regulator of murine dendritic cell homeostasis. Blood. 2013; 121:1016–27. [PubMed: 23212522]
16. Mildner A, Chapnik E, Varol D, Aychek T, Lampl N, Rivkin N, et al. MicroRNA-142 controls thymocyte proliferation. Eur J Immunol. 2017; 47:1142–52. [PubMed: 28471480]
17. Sun Y, Oravecz-Wilson K, Mathewson N, Wang Y, McEachin R, Liu C, et al. Mature T cell responses are controlled by microRNA-142. J Clin Invest. 2015; 125:2825–40. [PubMed: 26098216]
18. Yamada Y, Kosaka K, Miyazawa T, Kurata-Miura K, Yoshida T. miR-142-3p enhances FcepsilonRI-mediated degranulation in mast cells. Biochem Biophys Res Commun. 2014; 443:980–6. [PubMed: 24361879]
19. Chapnik E, Rivkin N, Mildner A, Beck G, Pasvolsky R, Metzl-Raz E, et al. miR-142 orchestrates a network of actin cytoskeleton regulators during megakaryopoiesis. Elife. 2014; 3:e01964. [PubMed: 24859754]
20. Rivkin N, Chapnik E, Birger Y, Yanowski E, Curato C, Mildner A, et al. Rac1 functions downstream of miR-142 in regulation of erythropoiesis. Haematologica. 2017
21. Rivkin N, Chapnik E, Mildner A, Barshtein G, Porat Z, Kartvelishvily E, et al. Erythrocyte survival is controlled by microRNA-142. Haematologica. 2017; 102:676–85. [PubMed: 27909218]
22. Lu X, Li X, He Q, Gao J, Gao Y, Liu B, et al. miR-142-3p regulates the formation and differentiation of hematopoietic stem cells in vertebrates. Cell Res. 2013; 23:1356–68. [PubMed: 24165894]
23. Jones M, Chase J, Brinkmeier M, Xu J, Weinberg DN, Schira J, et al. Ash1l controls quiescence and self-renewal potential in hematopoietic stem cells. J Clin Invest. 2015; 125:2007–20. [PubMed: 25866973]

24. Wu L, Cai C, Wang X, Liu M, Li X, Tang H. MicroRNA-142-3p, a new regulator of RAC1, suppresses the migration and invasion of hepatocellular carcinoma cells. FEBS Lett. 2011; 585:1322–30. [PubMed: 21482222]
25. Zheng Z, Ding M, Ni J, Song D, Huang J, Wang J. MiR-142 acts as a tumor suppressor in osteosarcoma cell lines by targeting Rac1. Oncol Rep. 2015; 33:1291–9. [PubMed: 25530132]
26. Lei Z, Xu G, Wang L, Yang H, Liu X, Zhao J, et al. MiR-142-3p represses TGF-beta-induced growth inhibition through repression of TGFbetaR1 in non-small cell lung cancer. FASEB J. 2014; 28:2696–704. [PubMed: 24558198]
27. Khvorova A, Reynolds A, Jayasena SD. Functional siRNAs and miRNAs exhibit strand bias. Cell. 2003; 115:209–16. [PubMed: 14567918]
28. Dahlhaus M, Roolf C, Ruck S, Lange S, Freund M, Junghanss C. Expression and prognostic significance of hsa-miR-142-3p in acute leukemias. Neoplasma. 2013; 60:432–8. [PubMed: 23581416]
29. Shrestha A, Carraro G, El Agha E, Mukhametshina R, Chao CM, Rizvanov A, et al. Generation and Validation of miR-142 Knock Out Mice. PLoS One. 2015; 10:e0136913. [PubMed: 26327117]
30. Cabezas-Wallscheid N, Klimmeck D, Hansson J, Lipka DB, Reyes A, Wang Q, et al. Identification of regulatory networks in HSCs and their immediate progeny via integrated proteome, transcriptome, and DNA methylome analysis. Cell Stem Cell. 2014; 15:507–22. [PubMed: 25158935]
31. Oguro H, Ding L, Morrison SJ. SLAM family markers resolve functionally distinct subpopulations of hematopoietic stem cells and multipotent progenitors. Cell Stem Cell. 2013; 13:102–16. [PubMed: 23827712]
32. Dykstra B, Kent D, Bowie M, McCaffrey L, Hamilton M, Lyons K, et al. Long-term propagation of distinct hematopoietic differentiation programs in vivo. Cell Stem Cell. 2007; 1:218–29. [PubMed: 18371352]
33. Colamaio M, Puca F, Ragozzino E, Gemei M, Decaussin-Petrucci M, Aiello C, et al. miR-142-3p down-regulation contributes to thyroid follicular tumorigenesis by targeting ASH1L and MLL1. J Clin Endocrinol Metab. 2015; 100:E59–69. [PubMed: 25238203]
34. Gregory GD, Vakoc CR, Rozovskaia T, Zheng X, Patel S, Nakamura T, et al. Mammalian ASH1L is a histone methyltransferase that occupies the transcribed region of active genes. Mol Cell Biol. 2007; 27:8466–79. [PubMed: 17923682]
35. Tanaka Y, Katagiri Z, Kawahashi K, Kioussis D, Kitajima S. Trithorax-group protein ASH1 methylates histone H3 lysine 36. Gene. 2007; 397:161–8. [PubMed: 17544230]
36. Zhu L, Li Q, Wong SH, Huang M, Klein BJ, Shen J, et al. ASH1L Links Histone H3 Lysine 36 Dimethylation to MLL Leukemia. Cancer Discov. 2016; 6:770–83. [PubMed: 27154821]
37. Tanaka Y, Kawahashi K, Katagiri Z, Nakayama Y, Mahajan M, Kioussis D. Dual function of histone H3 lysine 36 methyltransferase ASH1 in regulation of Hox gene expression. PLoS One. 2011; 6:e28171. [PubMed: 22140534]
38. Kats LM, Reschke M, Taulli R, Pozdnyakova O, Burgess K, Bhargava P, et al. Proto-oncogenic role of mutant IDH2 in leukemia initiation and maintenance. Cell Stem Cell. 2014; 14:329–41. [PubMed: 24440599]
39. Sasaki M, Knobbe CB, Munger JC, Lind EF, Brenner D, Brustle A, et al. IDH1(R132H) mutation increases murine haematopoietic progenitors and alters epigenetics. Nature. 2012; 488:656–9. [PubMed: 22763442]
40. Chaturvedi A, Araujo Cruz MM, Jyotsana N, Sharma A, Goparaju R, Schwarzer A, et al. Enantiomer-specific and paracrine leukemogenicity of mutant IDH metabolite 2-hydroxyglutarate. Leukemia. 2016; 30:1708–15. [PubMed: 27063596]
41. Chaturvedi A, Araujo Cruz MM, Jyotsana N, Sharma A, Yun H, Gorlich K, et al. Mutant IDH1 promotes leukemogenesis in vivo and can be specifically targeted in human AML. Blood. 2013; 122:2877–87. [PubMed: 23954893]
42. Lawrence HJ, Christensen J, Fong S, Hu YL, Weissman I, Sauvageau G, et al. Loss of expression of the Hoxa-9 homeobox gene impairs the proliferation and repopulating ability of hematopoietic stem cells. Blood. 2005; 106:3988–94. [PubMed: 16091451]

43. Thorsteinsdottir U, Mamo A, Kroon E, Jerome L, Bijl J, Lawrence HJ, et al. Overexpression of the myeloid leukemia-associated Hoxa9 gene in bone marrow cells induces stem cell expansion. Blood. 2002; 99:121–9. [PubMed: 11756161]

44. Bhattacharya A, Cui Y. SomamiR 2. 0: a database of cancer somatic mutations altering microRNA-ceRNA interactions. Nucleic Acids Res. 2016; 44:D1005–10. [PubMed: 26578591]

45. Buske C, Feuring-Buske M, Antonchuk J, Rosten P, Hogge DE, Eaves CJ, et al. Overexpression of HOXA10 perturbs human lymphomyelopoiesis in vitro and in vivo. Blood. 2001; 97:2286–92. [PubMed: 11290589]

46. Thorsteinsdottir U, Sauvageau G, Hough MR, Dragowska W, Lansdorp PM, Lawrence HJ, et al. Overexpression of HOXA10 in murine hematopoietic cells perturbs both myeloid and lymphoid differentiation and leads to acute myeloid leukemia. Mol Cell Biol. 1997; 17:495–505. [PubMed: 8972230]

47. Milne TA, Briggs SD, Brock HW, Martin ME, Gibbs D, Allis CD, et al. MLL targets SET domain methyltransferase activity to Hox gene promoters. Mol Cell. 2002; 10:1107–17. [PubMed: 12453418]

48. Spencer DH, Young MA, Lamprecht TL, Helton NM, Fulton R, O'Laughlin M, et al. Epigenomic analysis of the HOX gene loci reveals mechanisms that may control canonical expression patterns in AML and normal hematopoietic cells. Leukemia. 2015; 29:1279–89. [PubMed: 25600023]

49. Chen FF, Lou YJ, Chen J, Jin J, Zhou JN, Yin XF, et al. Absence of miR-142 mutation in Chinese patients with acute myeloid leukemia. Leuk Lymphoma. 2014; 55:2961–2. [PubMed: 24724784]

Significance

These findings provide mechanistic insights into the role of miRNAs in leukemogenesis and hematopoietic stem cell function.

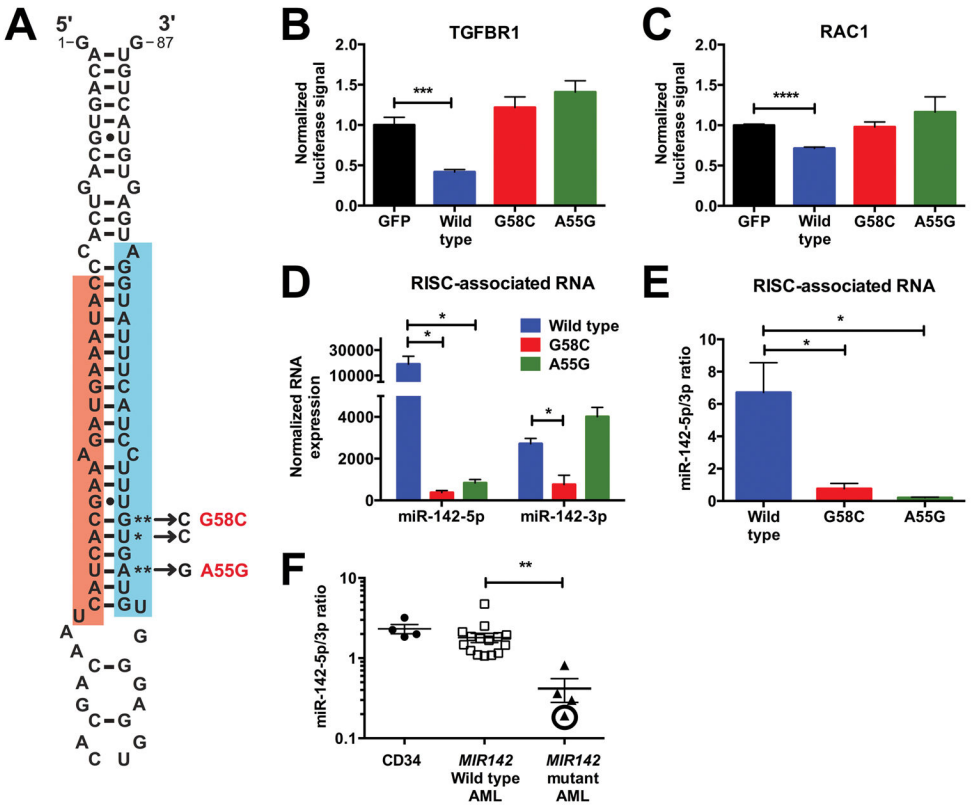

Figure 1. *MIR142* mutations attenuate miR-142-3p and miR-142-5p functions

a, MIR142 hairpin. Red: MiR-142-5p. Blue: MiR-142-3p. Mutations in the TCGA cohort are starred with G58C and A55G recurrently observed. **b–c,** Luciferase assays measuring the activity of wild type, G58C mutant, or A55G mutant MIR142 hairpins against the 3′ UTRs of *TGFBR1* (**b**) (n=4–5) and *RAC1* (**c**) (n=6). **d–e,** Total levels (**d**) and ratio (**e**) of RISC-associated miR-142-5p and miR-142-3p after overexpression of the wild type MIR142 hairpin (n=3) or of its G58C (n=3) and A55G (n=3) mutants. For **d**, normalized expression is defined as (number of reads mapped to a gene/total number of reads) x10^6. **f,** Ratio of miR-142-5p and miR-142-3p in normal donor $CD34^+$ cells, AML cells without *MIR142* mutations, and *MIR142* mutant AML cells. The circled data point was derived from an AML with bi-allelic *MIR142* mutations. Significance was determined with an unpaired t test. *P<0.05; **P<0.01; ***P<0.001; ****P<0.0001.

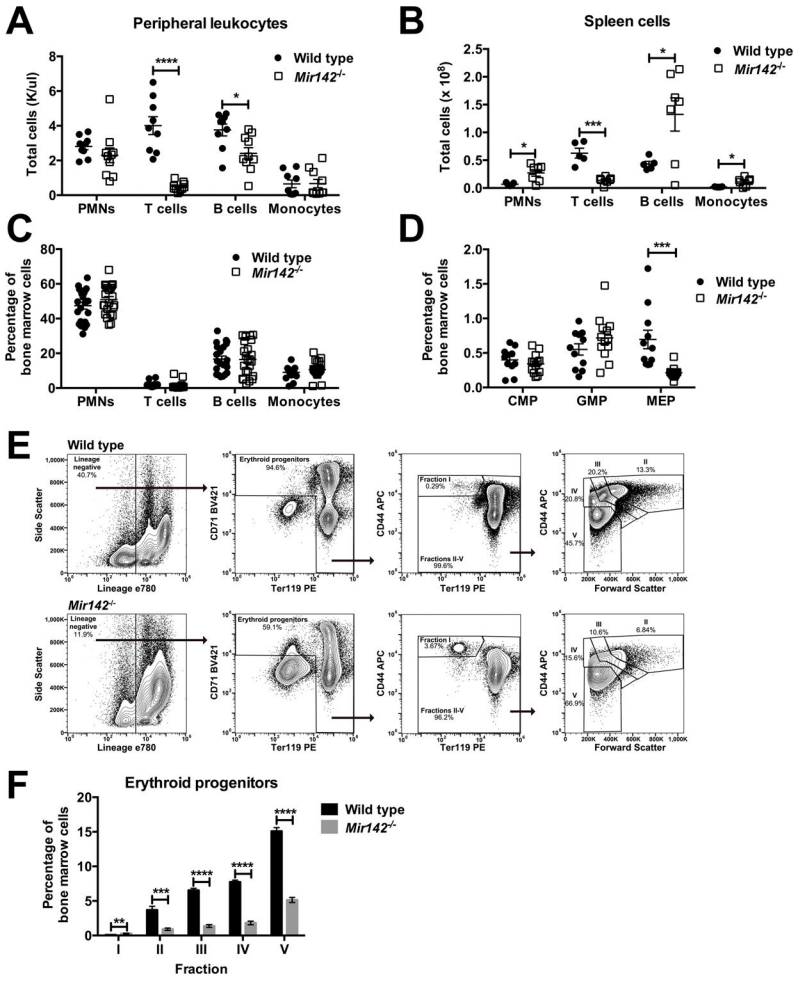

Figure 2. *Mir142* loss alters differentiation in mature hematopoietic populations

a–b, Number of cells for the indicated hematopoietic lineage in peripheral blood (**a**) and spleen (**b**). **c,** Percentage of mature hematopoietic cells in the bone marrow. PMNs: neutrophils. **d,** Percentage of CMPs, GMPs, or MEPs in the bone marrow. **e,** Representative flow plots of bone marrow erythroid progenitor analysis. **f,** Percentage of erythroid progenitors in *Mir142*$^{-/-}$ (n=5) bone marrow compared to control (n=5). Significance was determined with an unpaired t test. *P<0.05; **P<0.01; ***P<0.001; ****P<0.0001.

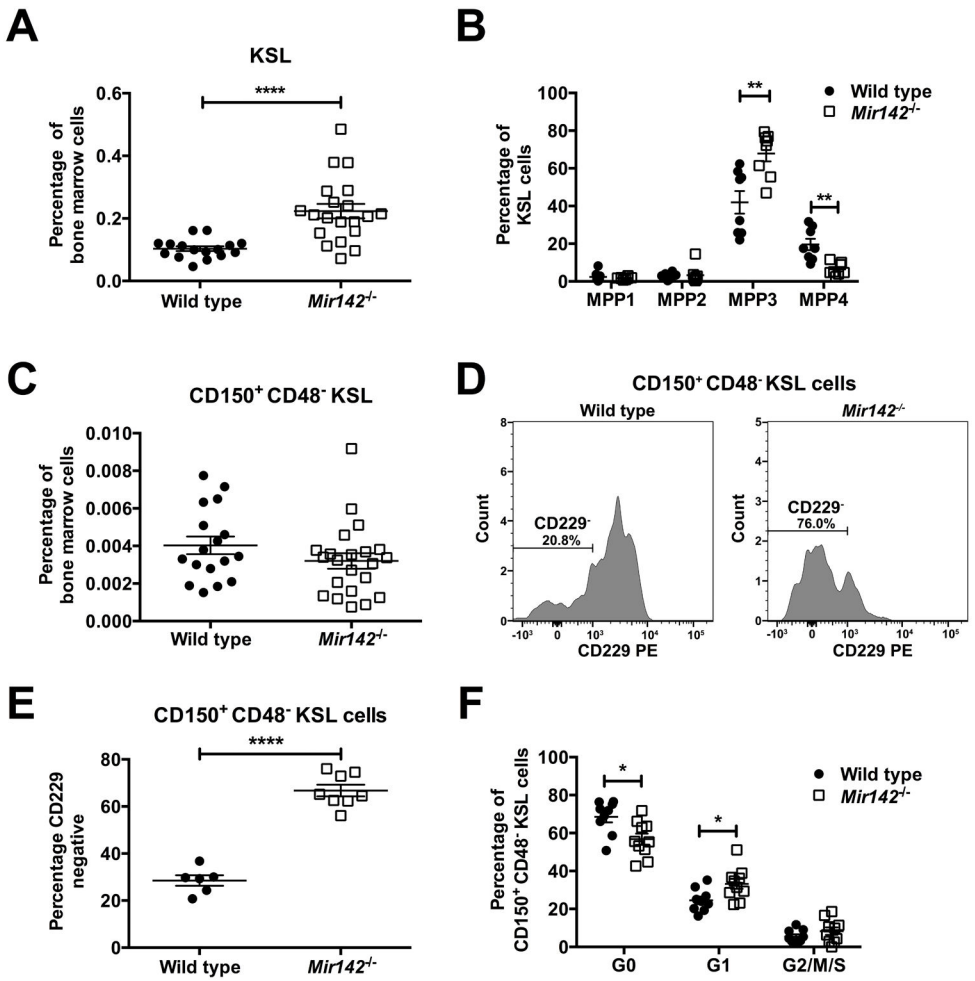

Figure 3. ***Mir142*** **loss alters differentiation in MPPs and HSCs**

a, Percentage of KSL cells in the bone marrow. **b,** Percentage of multipotent progenitors (MPP1, MPP2, MPP3, and MPP4 cells) within the KSL gate. **c,** Percentage of LT-HSCs ($CD150^{+}CD48^{-}$KSL cells) in the bone marrow. **d,** Representative histograms showing CD229 surface expression on LT-HSCs. **e,** $CD229^{-}$ cells as a percentage of bone marrow LT-HSCs. **f,** Cell cycle distribution of LT-HSCs. Significance was determined with an unpaired t test. *P<0.05; **P<0.01; ****P<0.0001.

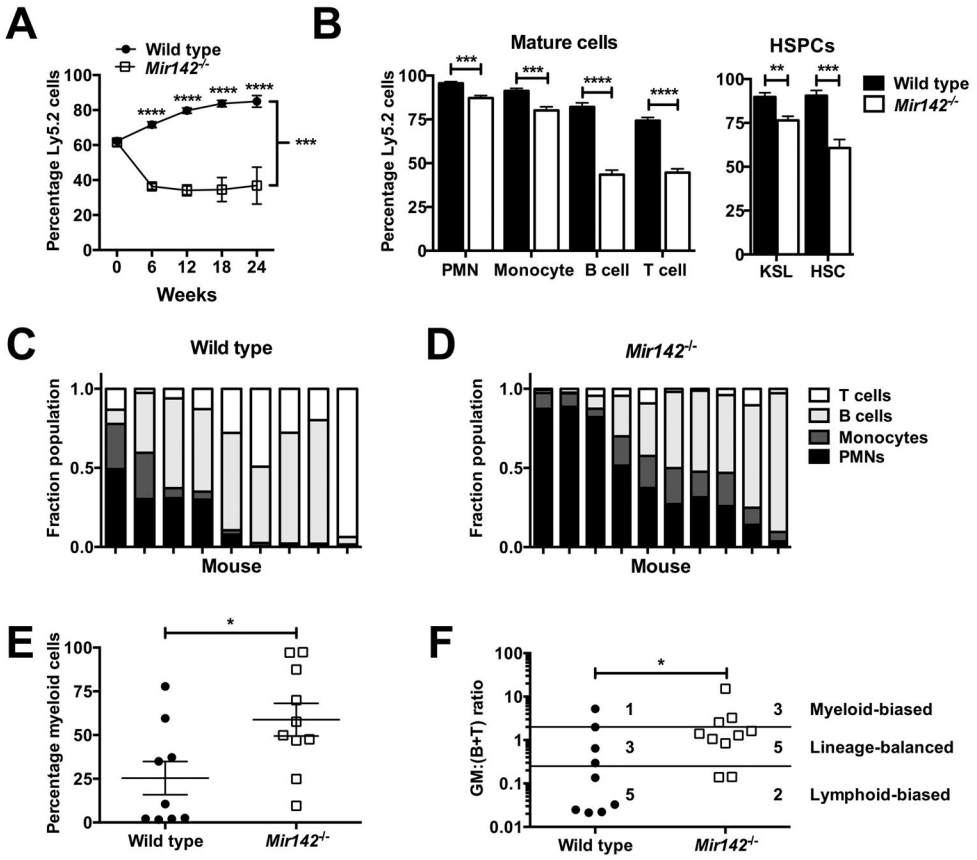

Figure 4. *Mir142*$^{-/-}$ bone marrow exhibits reduced repopulating activity with a loss of HSC lymphoid potential

a, Percentage donor (Ly5.2) chimerism in the peripheral blood following competitive transplantation of wild type or *Mir142*$^{-/-}$ bone marrow (week 0: input chimerism). Two independent experiments were performed with a combined total of 9–10 recipients per group. **b,** Percentage bone marrow donor chimerism 12 weeks post-transplantation (n = 5). KSL: Kit^{+}Sca^{+}Lin^{-} cells. HSC: CD150^{+}CD48^{-}KSL cells. **c**–**d**, Sorted donor CD150^{+}CD48^{-}KSL cells (20–25 per recipient) were transplanted into recipients in two independent experiments with peripheral blood donor chimerism assessed 24 weeks later. Shown is the contribution of the indicated lineage to the total donor cell pool in mice transplanted with wild type (**c**) or *Mir142*$^{-/-}$ (**d**) HSCs. Each column represents a mouse. **e,** Percentage of cells in **c** or **d** that were myeloid (Gr1^{+} or CD115^{+}). **f**, Quotient of the percentage donor contribution to the overall myeloid lineage (GM; Gr1^{+} or CD115^{+}) over the sum of the percentage donor contributions to the overall B and T cell lineages (B+T) for individual mice. Myeloid-biased mice had a ratio >2, lineage balanced mice between 0.25 and 2, and lymphoid-biased mice < 0.25. For **a**, significance was determined with a mixed-model analysis of covariance using input chimerism as a covariate. Pairwise differences were examined with Tukey-Kramer adjusted tests. Significance was determined with a two-way anova for **b**, with an unpaired t test for **e**, and with a Mann-Whitney test for **f**. *P<0.05; **P<0.01; ***P<0.001; ****P<0.0001.

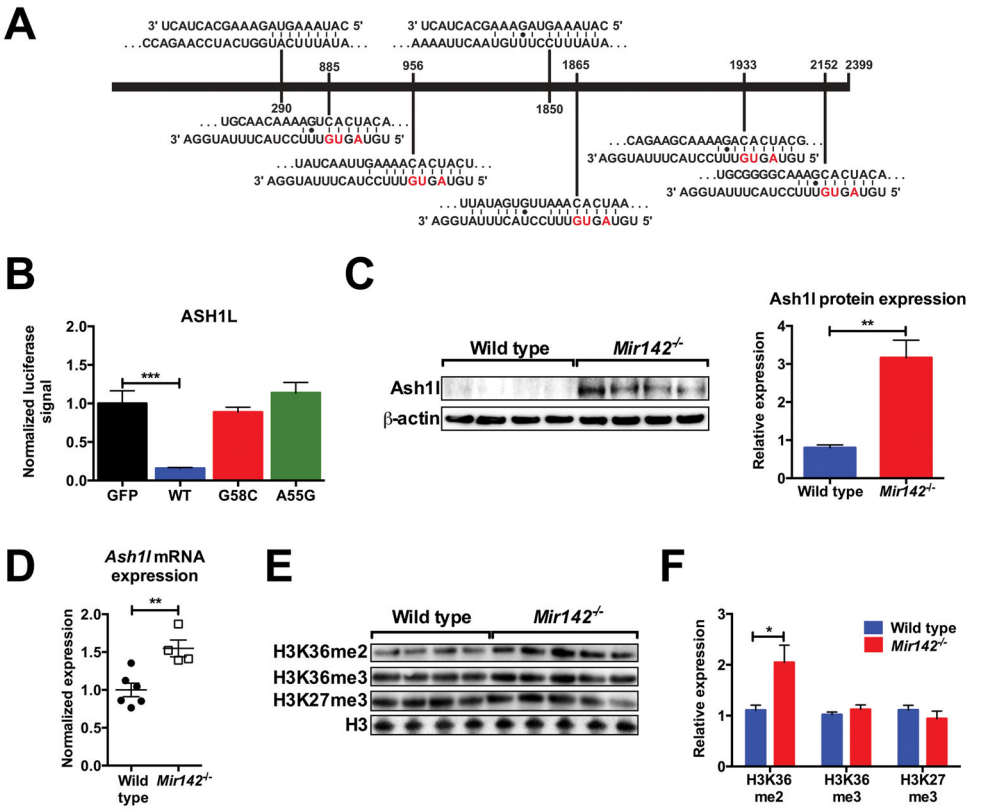

Figure 5. *Mir142* loss results in increased Ash1l activity

a, Predicted miR-142-5p (top) and miR-142-3p (bottom) target sites in the *ASH1L* 3′ UTR. Red: mutated in the TCGA cohort. **b,** Activity of wild type, G58C mutant, or A55G mutant MIR142 hairpins in luciferase assays against the *ASH1L* 3′ UTR (n=5). **c**, Western blot measuring Ash1l protein in wild type or *Mir142*$^{-/-}$ bone marrow cells. Quantification is to the right. **d**, *Ash1l* mRNA expression in c-kit^{+}-selected bone marrow cells normalized to wild type. **e**, Western blot measuring H3K36me2, H3K36me3, and H3K27me3 levels in c-kit^{+}-selected bone marrow cells. **f**, Quantification of **e**. Significance was determined with an unpaired t test. *P<0.05; **P<0.01; ***P<0.001.

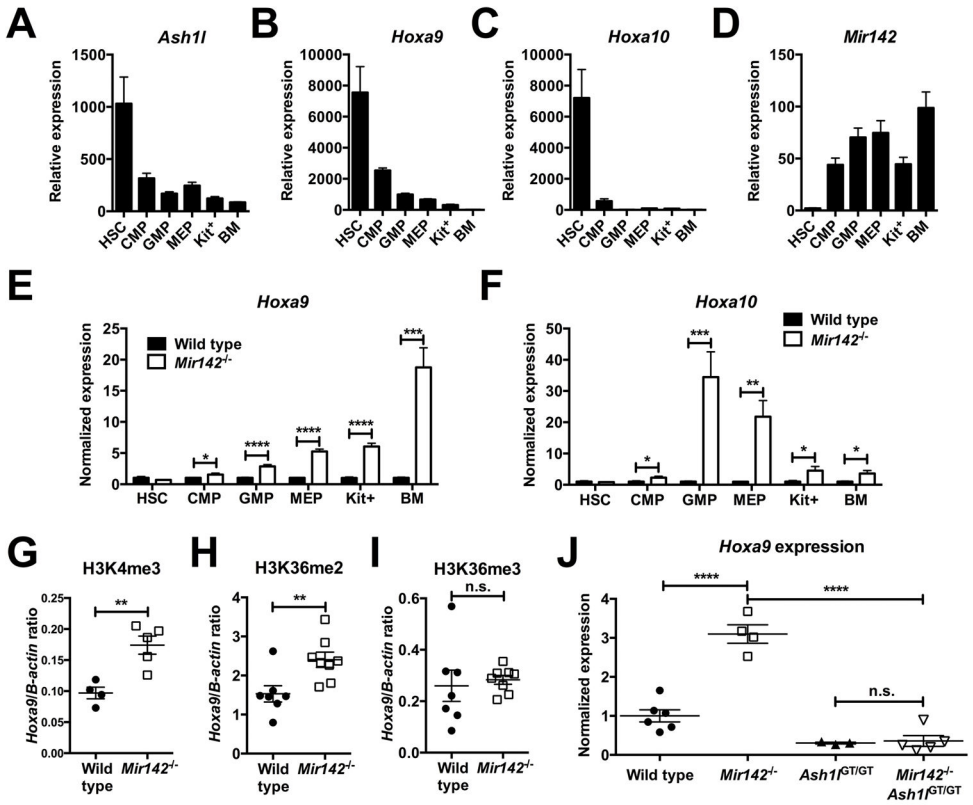

Figure 6. *Mir142* loss increases *Hoxa9/a10* expression through the derepression of Ash1l

a–**d,** RNA expression of *Ash1l* (**a**), *Hoxa9* (**b**), *Hoxa10* (**c**), and *Mir142-5p* (**d**) in the indicated hematopoietic cell populations in wild type mice (n=4–7). Kit^+: purified c-kit^+ bone marrow cells; BM: unselected bone marrow cells. For **a**–**c**, expression is relative to *Actb*. For **d**, expression is relative to *Sno202*. **e**–**f,** RNA expression of *Hoxa9* (**e**) and *Hoxa10* (**f**) in the indicated hematopoietic cell populations (n=4–7). Data are normalized to wild type. **g**–**i**, Ratio of cross-linked DNA at the *Hoxa9* promoter versus at the *β-actin* promoter pulled down with antibodies against H3K4me3 (**g**), H3K36me2 (**h**), or H3K36me3 (**i**). **j**, *Hoxa9* expression in total bone marrow cells. Data is normalized to wild type. Significance was determined with an unpaired t test. n.s. not significant. *P<0.05; **P<0.01; ***P<0.001; ****P<0.0001.

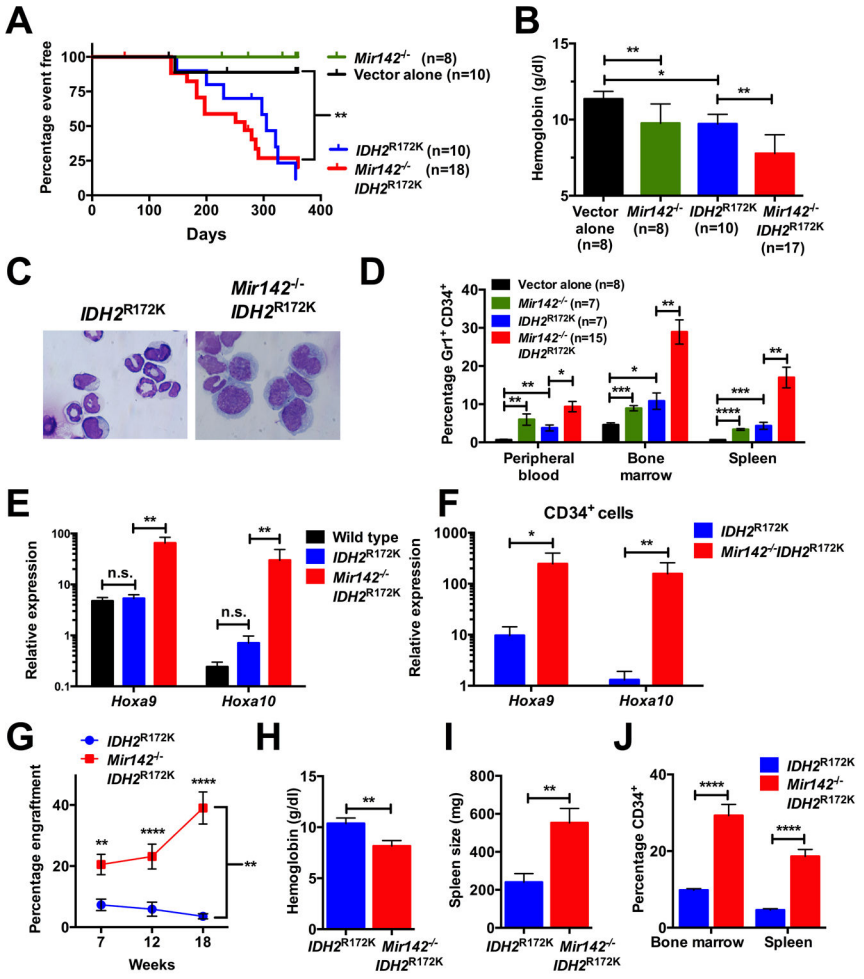

Figure 7. *Mir142* loss enhances *IDH2*^{R172K} disease initiating capacity

a–f, Mice were transplanted with wild type or *Mir142*$^{-/-}$ c-kit^{+} cells transduced with empty retrovirus (vector alone) or retrovirus expressing *IDH2*^{R172K}. **a,** Mouse survival. Mice were sacrificed if distressed or if their hemoglobin was < 5 g/dl. Mice sacrificed for non-hematologic reasons were censored. **b,** Hemoglobin twenty weeks post-transplantation. **c,** Representative bone marrow cytospins. **d,** Percentage of Gr-1^{+}CD34^{+} cells in the peripheral blood, bone marrow, or spleen upon sacrifice. **e–f,** *Hoxa9/a10* RNA expression in total bone marrow (**e**) or sorted CD34^{+} (**f**) cells upon sacrifice (n=4–6). Expression is relative to *Actb*. **g–j,** 1x10^{6} splenocytes from *IDH2*^{R172K} or *Mir142*$^{-/-}$*IDH2*^{R172K} primary recipient mice were transplanted into sublethally irradiated secondary recipients. Four *IDH2*^{R172K} and five *Mir142*$^{-/-}$*IDH2*^{R172K} donors were separately transplanted into 3–7 recipients, with 20 and 25 recipients respectively analyzed. Shown are the donor chimerism in peripheral blood (**g**), hemoglobin 18 weeks post-transplantation (**h**), and the spleen size (**i**) and percentage of CD34^{+} cells in the bone marrow and spleen (**j**) upon sacrifice. Significance was determined with a Mantel-Cox log rank test for **a**, with an unpaired t test for **b**, **d**, and **h–j**, and with a Mann-Whitney test for **e–f**. For **g**, significance was determined with a mixed-model analysis of variance using log (percent engraftment) as the dependent variable. Pairwise differences

were examined with Tukey-Kramer adjusted tests. n.s. not significant. *P<0.05; **P<0.01; ***P<0.001; ****P<0.0001.